molecular pharmaceutics

articles

Analysis of the Thermal and pH Stability of Human Respiratory Syncytial Virus

Salvador F. Ausar,[†] Jason Rexroad,[†] Vladimir G. Frolov,[‡] Jee L. Look,[‡] Nandini Konar,[‡] and C. Russell Middaugh*,[†]

Department of Pharmaceutical Chemistry, University of Kansas, 2095 Constant Avenue, Lawrence, Kansas 66047, and Wyeth Vaccines Research, 401 North Middletown Road, Pearl River, New York 10965

Received June 1, 2005

Abstract: Respiratory syncytial virus (RSV) was studied as a function of pH (3−8) and temperature (10−85 °C) by fluorescence, circular dichroism, and high-resolution second-derivative absorbance spectroscopies, as well as dynamic light scattering and optical density as a measurement of viral aggregation. The results indicate that the secondary, tertiary, and quaternary structures of RSV are both pH and temperature labile. Derivative ultraviolet absorbance and fluorescence spectroscopy (intrinsic and extrinsic) analyses suggest that the stability of tertiary structure of RSV proteins is maximized near neutral pH. In agreement with these results, the secondary structure of RSV polypeptides seems to be more stable at pH 7−8, as evaluated by circular dichroism spectroscopy. The integrity of the viral particles studied by turbidity and dynamic light scattering also revealed that RSV is more thermally stable near neutral pH and particularly prone to aggregation below pH 6. By combination of the spectroscopic data employing a multidimensional eigenvector phase space approach, an empirical phase diagram for RSV was constructed. The pharmaceutical utility of this approach and the optimal formulation conditions are discussed.

Keywords: RSV thermostability; absorption spectroscopy; biophysical models; circular dichroism; fluorescence spectroscopy; dynamic light scattering; vaccine formulation

Introduction

Human respiratory syncytial virus (RSV) is the leading cause of lower respiratory tract infections (i.e., bronchiolitis and pneumonia) among young children worldwide. In addition, RSV is a leading cause of hospitalization in adults with community-acquired respiratory disease.[1−5] In the United States alone RSV causes an estimated 51 000 to 82 000 hospitalizations annually.[6] The regularity of RSV outbreaks and the frequency of reinfection demonstrate the significant disease threat that RSV imposes throughout life and the need for disease prophylaxis.

* To whom correspondence should be addressed. Mailing address: Department of Pharmaceutical Chemistry, University of Kansas, 2095 Constant Ave., Lawrence, KS 66047. Tel: (785)864-5813. Fax: (785)864-5814. E-mail: middaugh@ku.edu.

[†] University of Kansas.

[‡] Wyeth Vaccines Research.

(1) Dowell, S. F.; Anderson, L. J.; Gary, H. E., Jr.; Erdman, D. D.; Plouffe, J. F.; File, T. M., Jr.; Marston, B. J.; Breiman, R. F. Respiratory syncytial virus is an important cause of community-acquired lower respiratory infection among hospitalized adults. *J. Infect. Dis.* **1996**, *174*, 456−462.

(2) Falsey, A. R.; McCann, R. M.; Hall, W. J.; Tanner, M. A.; Criddle, M. M.; Formica, M. A.; Irvine, C. S.; Kolassa, J. E.; Barker, W. H.; Treanor, J. J. Acute respiratory tract infection in daycare centers for older persons. *J. Am. Geriatr. Soc.* **1995**, *43*, 30−36.

(3) La Montagne, J. R. RSV pneumonia, a community-acquired infection in adults. *Lancet* **1997**, *349*, 149−150.

(4) Marx, A.; Gary, H. E., Jr.; Marston, B. J.; Erdman, D. D.; Breiman, R. F.; Torok, T. J.; Plouffe, J. F.; File, T. M., Jr.; Anderson, L. J. Parainfluenza virus infection among adults hospitalized for lower respiratory tract infection. *Clin. Infect. Dis.* **1999**, *29*, 134−140.

(5) Nicholson, K. G. Impact of influenza and respiratory syncytial virus on mortality in England and Wales from January 1975 to December 1990. *Epidemiol. Infect.* **1996**, *116*, 51−63.

10.1021/mp0500465 CCC: $30.25
Published on Web 09/14/2005

Despite more than 40 years of research, effective methods to control RSV infections have proven elusive. The development of a vaccine against RSV has been complicated by the lack of a robust immune response (even after natural infection)[1,2] and the diversity and omnipresence of populations at risk for infection. During the mid-1960s, a formalin-inactivated RSV vaccine was tested, but it met with failure. Not only did this vaccine fail to provide protection against disease, but it also enhanced the disease state during subsequent natural infection with RSV and increased the incidence of pneumonia and bronchiolitis.[7,8] Currently, the most effective method of RSV disease prophylaxis is via passive immunization with high levels of RSV-specific antibodies that must be administered as a monthly injection. In addition to being extremely costly and inconvenient, this method is not practical, given the increasing number of high-risk infants.[9]

To date, live attenuated vaccines are the most promising type of vaccine against RSV since an enhanced disease state has never been observed following natural infection after the administration of this form of RSV vaccine. Furthermore, live attenuated vaccines afford better immune protection in general compared to killed or subunit vaccines. Recent efforts suggest that an effective recombinant live attenuated RSV vaccine may be possible,[10] but the development of an efficacious viral vaccine for worldwide distribution will be challenging, especially when the labile nature[11,12] and complex structure of RSV are considered. RSV is an enveloped single-stranded, negative-sense RNA virus of the family *Paramyxoviridae*.[12] The RSV genome consists of approximately 15 222 nucleotides which encodes 10 proteins, 2 of which are nonstructural. Virions are irregular in shape and range from 100 to 300 nm in diameter.[12]

Their reported lability and heterogeneous size represent significant obstacles to the characterization and formulation of a stable RSV vaccine. The employment of a comprehensive biophysical characterization approach, however, with the potential to elucidate the pathways of thermally induced physical degradation should provide information that is relevant to the rational design of a stable RSV vaccine formulation. Although studies of the effect of pH and temperature on the biological activity of RSV have been conducted,[13,14] efforts to determine the effect of pH and temperature on the physical structure of RSV have not been performed. To this end, we have employed a variety of biophysical techniques to study the thermal stability of RSV as a function of pH. In addition, by employing a multidimensional eigenvector phase space approach,[15] we incorporate the data from these studies into an empirical phase diagram (EPD). The EPD illustrates the physical stability of RSV under a variety of conditions (i.e., pH and temperature) and identifies regions where structural integrity is maintained and lost. Thus, the EPD provides an intuitive picture of the physical stability of RSV and a foundation for formulation studies since stabilization against the degradation pathways identified in these studies should yield a more thermally stable vaccine.

Experimental Section

RSV Purification. Human respiratory syncytial virus (RSV) strain rA39 was obtained from Wyeth. RSV particles were isolated by employing a discontinuous 30/60% sucrose gradient in NTE buffer and subsequently concentrated by centrifugation over a 1.45 M sucrose cushion as previously reported.[16] The virus band was collected and dialyzed overnight at 4 °C against 20 mM citrate/phosphate buffer at the appropriate pH (range pH 3−8 in 1 unit intervals). To determine virus particle concentration, an ELISA sandwich assay was employed using the method of Malley et al.[17] Briefly, 96-well flat bottom plates were coated with

(6) Shay, D. K.; Holman, R. C.; Newman, R. D.; Liu, L. L.; Stout, J. W.; Anderson, L. J. Bronchiolitis-associated hospitalizations among US children, 1980−1996. *JAMA, J. Am. Med. Assoc.* **1999**, *282*, 1440−1446.

(7) Kapikian, A. Z.; Mitchell, R. H.; Chanock, R. M.; Shvedoff, R. A.; Stewart, C. E. An epidemiologic study of altered clinical reactivity to respiratory syncytial (RS) virus infection in children previously vaccinated with an inactivated RS virus vaccine. *Am. J. Epidemiol.* **1969**, *89*, 405−421.

(8) Kim, H. W.; Canchola, J. G.; Brandt, C. D.; Pyles, G.; Chanock, R. M.; Jensen, K.; Parrott, R. H. Respiratory syncytial virus disease in infants despite prior administration of antigenic inactivated vaccine. *Am. J. Epidemiol.* **1969**, *89*, 422−434.

(9) Leader, S.; Kohlhase, K. Recent trends in severe respiratory syncytial virus (RSV) among US infants, 1997 to 2000. *J. Pediatr.* **2003**, *143* (Suppl. 5), 127−132.

(10) Karron, R. A.; Wright, P. F.; Belshe, R. B.; Thumar, B.; Casey, R.; Newman, F.; Polack, F. P.; Randolph, V. B.; Deatly, A.; Hackell, J.; Gruber, W.; Murphy, B. R.; Collins, P. L. Identification of a recombinant live attenuated respiratory syncytial virus vaccine candidate that is highly attenuated in infants. *J. Infect. Dis.* **2005**, *191*, 1093−1104.

(11) Beem, M.; Wright, F. H.; Hamre, D.; Egerer, R.; Oehme, M. Association of the chimpanzee coryza agent with acute respiratory disease in children. *N. Engl. J. Med.* **1960**, *263*, 523−530.

(12) Collins, P. L.; McIntosh, K.; Chanock, R. M. Respiratory Syncytial Virus. In *Fields Virology*, 3rd ed.; Fields, B. N., Knipe, D. M., Howley, P. M., Eds.; Lippincott-Raven Publisher: Philadelphia, 1995; pp 1313−1351.

(13) Hambling, M. H. Survival of The Respiratory Syncytial Virus During Storage Under Various Conditions. *Br. J. Exp. Pathol.* **1964**, *45*, 647−655.

(14) Rechsteiner, J. Inactivation of respiratory syncytial virus in air. *Antonie Van Leeuwenhoek* **1969**, *35*, 238.

(15) Kueltzo, L. A.; Ersoy, B.; Ralston, J. P.; Middaugh, C. R. Derivative absorbance spectroscopy and protein phase diagrams as tools for comprehensive protein characterization: a bGCSF case study. *J. Pharm. Sci.* **2003**, *92*, 1805−1820.

(16) Ueba, O. Respiratory syncytial virus. I. Concentration and purification of the infectious virus. *Acta Med. Okayama* **1978**, *32*, 265−272.

(17) Malley, R.; Vernacchio, L.; Devincenzo, J.; Ramilo, O.; Dennehy, P. H.; Meissner, H. C.; Gruber, W. C.; Jafri, H. S.; Sanchez, P. J.; Macdonald, K.; Montana, J. B.; Thompson, C. M.; Ambrosino, D. M. Enzyme-linked immunosorbent assay to assess respiratory syncytial virus concentration and correlate results with inflammatory mediators in tracheal secretions. *Pediatr. Infect. Dis. J.* **2000**, *19*, 1-7.

100 μL/well of unconjugated goat anti-RSV polyclonal antibody (Fitzgerald) and incubated at room temperature for 3 h. Plates were washed five times with PBS and blocked for 1.5 h with PBS−BSA (5% w/v). Standards and virus were plated in triplicate with 12 2-fold serial dilutions made in 1% PBS−BSA, incubated for 3 h at room temperature, and washed five times with PBS. Peroxidase-conjugated goat anti-RSV polyclonal antibody was added, incubated for 1.5 h at room temperature, and washed five times with PBS. The liquid substrate 3,3′,5,5′-tetramethylbenzidine (100 μL/well; Sigma) was added to each well and incubated for 30 min at room temperature. The reaction was stopped with 100 μL/well 1 N HCl, and the absorbance at 450 nm was recorded employing a plate reader (BMG Labtechnologies, Offenburg, Germany). A stock solution of RSV type A/Long strain containing 6×10^5 PFU/mL from ATCC was used for ELISA standardization. The protein concentration of the virus suspension was determined using a BCA protein assay kit as described by the manufacturer (Pierce).

UV Absorbance Spectroscopy. UV absorption spectra of RSV (0.3 mg/mL protein) were obtained in 2.5 °C increments from 10 to 85 °C at each pH over the range 3−8 employing an Agilent 8453 diode-array spectrophotometer as previously described.[18] Studies were conducted in capped quartz cells. In addition, the optical density at 350 nm (turbidity) was monitored over the same temperature range to assess the aggregation behavior of RSV.

Fluorescence Spectroscopy. Intrinsic fluorescence spectroscopy studies were performed in a PTI Quanta Master fluorometer equipped with a Peltier temperature control device to assess the stability of the tertiary structure of the RSV proteins. RSV samples (0.17 mg/mL protein) were contained in capped quartz cells in a 4-position turret. Samples were excited at 290 nm, and emission spectra were collected from 10 to 85 °C in 2.5 °C intervals employing excitation and emission slits of 4 nm. A 5 min equilibration time was used at each temperature. The spectrum of the buffer was obtained at each temperature and subtracted from the sample spectrum at each corresponding temperature. To further investigate the stability of the RSV proteins, samples (0.17 mg/mL protein) in the presence of 6 μM 8-anilino-1-naphthalene sulfonate (ANS) were excited at 385 nm and the emission spectra of the dye were monitored from 400 to 580 as a function of the temperature. Excitation and emission slits were set at 5 nm, and a 5 min hold time was used at each temperature prior to data collection. Emission spectra of 6 μM ANS in buffer alone were subtracted from sample spectra at each temperature.

Circular Dichroism Spectroscopy. Circular dichroism spectroscopy (CD) studies were performed employing a Jasco-810 spectropolarimeter (Tokyo, Japan) equipped with a Peltier temperature control device and a six-position sample holder. CD spectra of virus samples (0.35 mg/mL protein) were collected at a scanning speed of 10 nm/s and a resolution of 0.2 nm, over the range 190−260 nm. Additionally, the CD signal at 222 nm was recorded with increasing temperature from 10 to 85 °C using a 15 °C/h temperature ramp rate.

Dynamic Light Scattering. The size of RSV as a function of temperature was monitored by dynamic light scattering. A stock solution of RSV was diluted in 20 mM citrate−phosphate buffer at the appropriate pH and filtered through 0.45 μm filters. Measurements were recorded every 2.5 °C from 10 to 90 °C in a light scattering instrument (Brookhaven Instrument Corp., Holtzille, NY) equipped with a 50 mW diode-pumped laser ($\lambda = 532$ nm). The scattered light was monitored at 90° to the incident beam, and the autocorrelation function was generated via a digital generator (BI-9000AT). The effective hydrodynamic diameter was calculated from the diffusion coefficient by the Stokes−Einstein equation using the method of cumulants. Data were collected continuously for five 30 s intervals for each sample and plotted as the mean hydrodynamic diameter with accompanying standard error.

Empirical Phase Diagram (EPD). The EPD was generated using data points at 2.5° intervals from 10 to 85° C. The data used to construct the EPD are as follows: all six second-derivative UV peaks, CD at 222 nm, optical density at 350 nm, intrinsic fluorescence peak position, intrinsic fluorescence peak position intensity, and ANS fluorescence intensity at 485 nm. The data generated by the various biophysical techniques employed were initially ordered by parameter (i.e., pH and temperature) in Microsoft Word and copied into Mathematica version 4.2 (Wolfram Research, Inc.) for phase diagram preparation. The discrete parameters are analogous to coordinates that are associated with a set of variables from each technique employed. These variables represent unit vectors that define an *n*-dimensional vector space with dimensions equal to the number of variables included in the data set. Individual unit vector projectors are then calculated and summed to obtain a density matrix. The eigenvalues and eigenvectors of the density matrix are calculated, and the most influential three components are represented as colors in a RGB-based (red, green, or blue) scheme. Finally, the three components are summed to yield a final color that represents the physical state of the virus under those conditions (i.e., temperature and pH). Thus, the EPD represents the physical stability of RSV as a multicomponent vector with the components defined by measurements indicated. A more detailed description of this method can be found elsewhere.[15]

Results

UV Spectroscopy. The UV absorption spectrum of RSV at 10 °C and neutral pH manifests a maximum in the optical density near 269 nm suggesting that both the RNA core and the viral proteins contribute significantly to the spectrum (Figure 1, solid line). The spectrum shown in Figure 1 also contains a significant light scattering component since the optical density does not return to baseline above 300 nm.

(18) Rexroad, J.; Wiethoff, C. M.; Green, A. P.; Kierstead, T. D.; Scott, M. O.; Middaugh, C. R. Structural stability of adenovirus type 5. *J. Pharm. Sci.* **2003**, *92*, 665−678.

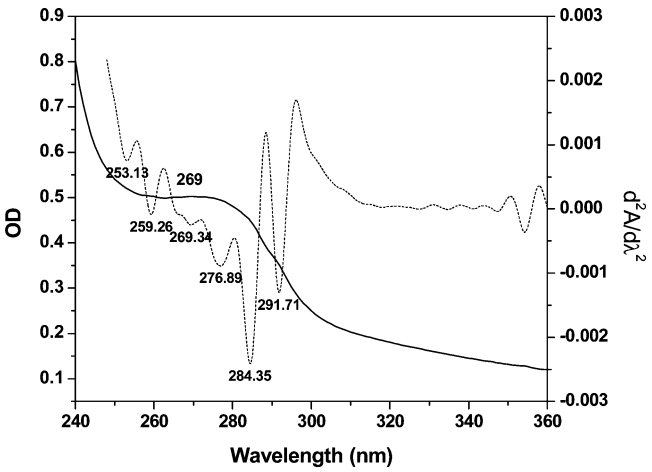

Figure 1. Representative UV optical density spectrum of RSV (solid line) and its second derivative (dotted line). The spectrum was obtained at a viral protein concentration of 0.3 mg/mL at 10 °C, pH 7.

This presumably reflects the relatively large size of RSV particles. The second derivative of the RSV optical density spectrum (Figure 1, dotted line) possesses three negative peaks above 270 nm which correspond to light absorbed by the aromatic amino acids tyrosine (peak near 276 nm), a combination of tyrosine and tryptophan (peak near 284 nm), and tryptophan (peak near 292 nm).[19−21] Although phenylalanine (Phe) residues absorb light below 270 nm, the negative peaks between 253 and 270 nm cannot be definitively assigned due to the spectral overlap of Phe and the RNA genome of RSV. The sharpness of these peaks, however, suggests that they may originate from the Phe side chains since purine and pyrimidine absorbance peaks are typically broad.

If the degree of solvent exposure of the aromatic amino acid side chains changes with temperature, shifts in the negative peak positions are expected to occur. In general, absorbance peak positions shift to lower wavelengths when aromatic residues become more solvent exposed while shifts to higher wavelength imply that the solvent environments of the aromatic amino acid side chains are becoming more apolar. Similar red shifts are often seen as a consequence of protein aggregation. Plots of the negative absorbance peak positions of RSV versus temperature suggest that the tertiary structure of the virus is more thermally stable near neutral pH, with maximal stability observed at pH 7 (Figure 2). Peak

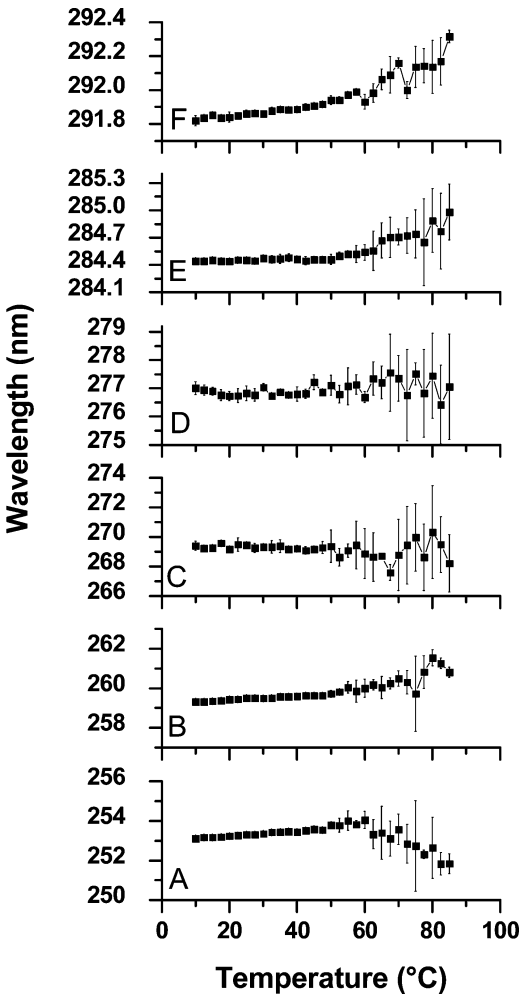

Figure 2. High-resolution second-derivative UV spectroscopy negative peak positions as a function of temperature for RSV at pH 7 with standard errors of the mean ($n = 3$). Peaks below 270 nm (A, B, and C) cannot be definitively assigned due to the overlapping absorbance of Phe and the RNA core. Peaks near 277 nm (D), 284 nm (E), and 292 nm (F) are attributed to the absorbance of Tyr, a combination of Tyr/Trp and Trp, respectively.

positions remain relatively constant with temperature at pH 6 (not shown) and 7 up to approximately 45 and 50 °C, respectively, suggesting that the tertiary structure of the RSV proteins undergoes negligible changes up to these temperatures. Although the data are quite noisy at higher temperatures, the general trend in the shifts of the Tyr and Tyr/Trp peak positions is to higher wavelengths, suggesting that the aromatic residues within the RSV proteins are becoming less solvent exposed. At pH 3−5, however, RSV undergoes significant aggregation during dialysis as a result of the altered charge state of the RSV proteins. The self-associated state of RSV complicates data reproducibility and interpretation although peak positions can still be determined due to the derivative nature of the analysis.

This aggregation is confirmed by the elevated OD values at 10 °C observed below pH 6, again suggesting that the RSV proteins are particularly sensitive to aggregation upon

(19) Mach, H.; Middaugh, C. R. Simultaneous monitoring of the environment of tryptophan, tyrosine, and phenylalanine residues in proteins by near-ultraviolet second-derivative spectroscopy. *Anal. Biochem.* **1994**, *222*, 323−331.

(20) Mach, H.; Thomson, J. A.; Middaugh, C. R. Quantitative analysis of protein mixtures by second derivative absorption spectroscopy. *Anal. Biochem.* **1989**, *181*, 79−85.

(21) Mach, H.; Thomson, J. A.; Middaugh, C. R.; Lewis, R. V. Examination of phenylalanine microenvironments in proteins by second-derivative absorption spectroscopy. *Arch. Biochem. Biophys.* **1991**, *287*, 33−40.

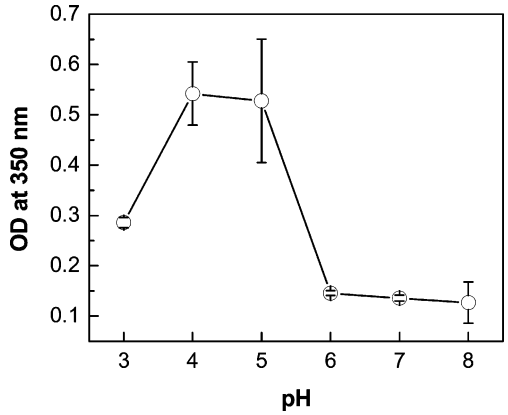

Figure 3. Optical density at 350 nm of RSV at 10 °C with standard errors of the mean ($n = 3$). Viral protein concentration was approximately 0.3 mg/mL.

exposure to acidic conditions (Figure 3). Furthermore, an increase in the OD of RSV is observed with increasing temperature at pH 4 and 5 up to approximately 27 and 32 °C, respectively, at which point a decrease in the OD is observed presumably due to precipitation of the samples.

The OD of RSV at pH 6−8 after dialysis, however, is relatively low (<0.2), and increases in scattered light are seen near the temperatures at which structural changes are detected by second-derivative analysis (Figure 4). Together, the derivative UV absorbance and turbidity data suggest that the structural stability is maximized near neutral pH. Additionally, multiple structural phenomena (e.g., changes in the degree of solvent exposure of the aromatic side chains, aggregation, etc.) which also reflect the heterogeneity of the macromolecular structure of RSV appear take place above 40 °C since data reproducibility is poor at higher temperatures.

Intrinsic Fluorescence Spectroscopy. Intrinsic and extrinsic fluorescence spectroscopies were employed with increasing temperature to further investigate the tertiary structural stability of the RSV proteins. By monitoring changes in intrinsic fluorescence peak position and fluorescence emission intensity, changes in the tertiary structure of the viral proteins can often be detected. In general, shifts in peak position to longer wavelengths with increases in temperature suggest that the average environment of the tryptophan residues is becoming more polar as a result of thermally induced perturbation in the tertiary structure of viral proteins. Conversely, shifts to shorter wavelengths generally indicate that the environment of the Trp residues is becoming more apolar. Shifts to shorter wavelengths are often observed upon protein aggregation. Note that these shifts are opposite to those seen in absorbance measurements. Similar to the results obtained by second-derivative UV spectroscopy, however, intrinsic fluorescence data suggests that the tertiary structure of the RSV proteins is relatively labile at pH 4 and 5 (Figure 5) since shifts in peak positions to higher wavelengths are observed at relatively low temperatures (near 32 and 40 °C, respectively). These shifts to higher wavelengths suggest that

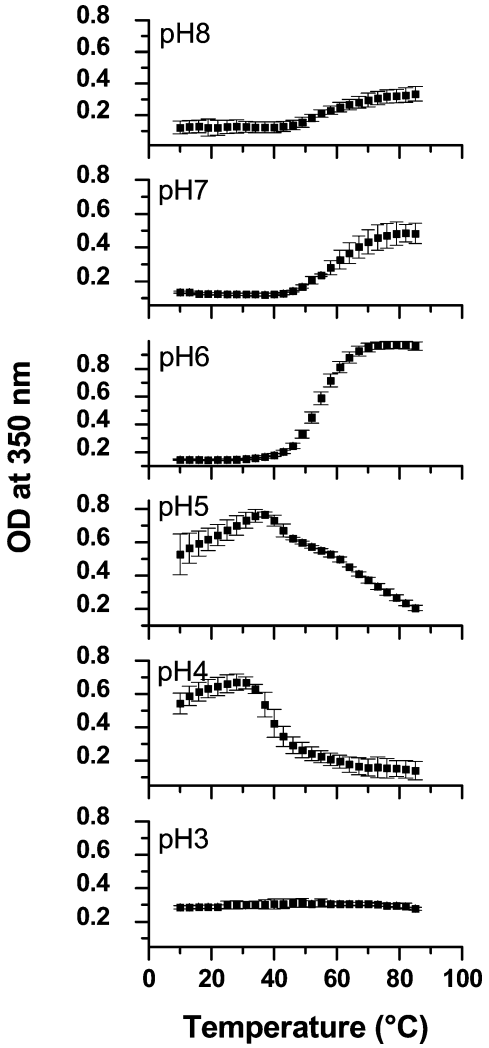

Figure 4. Optical density at 350 nm (OD) versus temperature for RSV (0.3 mg/mL protein) at pH 3−8 ($n = 3$).

changes in tertiary structure result in at least partial exposure of the Trp residues to the aqueous solvent. The exposure of the apolar Trp residues probably also leads to aggregation of the RSV particles since the temperature at which these changes in tertiary structure are detected correlate with the temperatures at which increases in turbidity occur (Figure 4).

Contrary to the UV absorbance spectroscopic studies, however, intrinsic fluorescence data suggests that the tertiary structure of RSV at pH 3 and 8 is stable to approximately 50 °C since shifts in peak position are not observed below this temperature. Shifts in the peak positions to lower wavelengths suggest that the Trp residues become incorporated into a less solvent exposed environment above 50 °C. In total, these results along with the absorbance and turbidity studies suggest that the RSV proteins undergo aggregation near the temperature at which shifts in peak positions are observed.

Extrinsic Fluorescence Spectroscopy. Extrinsic fluorescence spectroscopy was performed using the amphipathic fluorescent probe ANS. The fluorescence of ANS is strongly

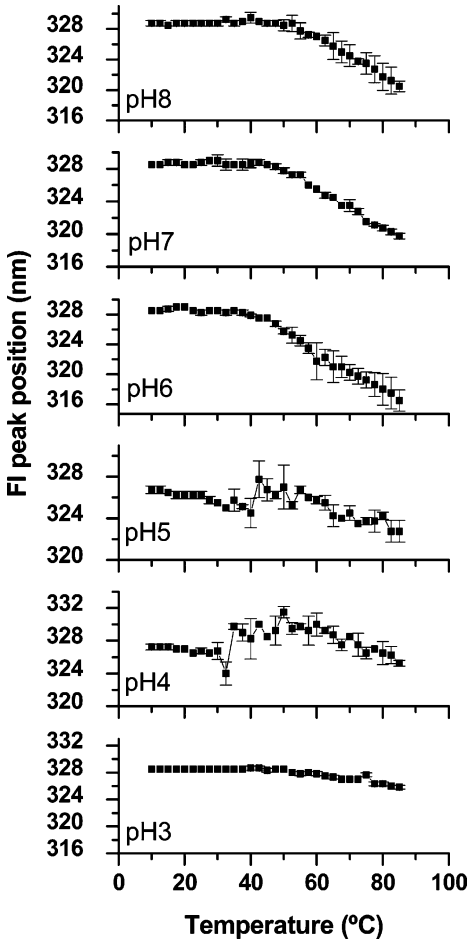

Figure 5. Intrinsic fluorescence (Trp) peak position versus temperature for RSV (0.17 mg/mL protein) at pH 3−8 ($n = 3$).

quenched when free in aqueous solution. Its fluorescence intensity is enhanced and blue shifted, however, when the dye is incorporated into a more apolar environment. Thus, by monitoring the fluorescence of ANS, changes in the tertiary structure of the viral proteins can often be detected. Data obtained by this method again suggest that the tertiary structure of the RSV proteins is most stable near neutral pH since increases in the fluorescence intensity of ANS occur at higher temperatures under neutral conditions compared to the other pH values studied (Figure 6). Additionally, analysis of the structural stability of the RSV proteins by this technique suggests that the virus is especially labile below pH 6. Marked decreases in ANS fluorescence intensity are detected near 25 °C at pH 4 and 5, while a more linear temperature-dependent decrease in fluorescence intensity is observed at pH 3 up to approximately 50 °C. The dramatic drops in ANS fluorescence intensity at pH 4 and 5 again probably reflect aggregation and precipitation of the virus since transition temperatures correlate well with decreases in OD at these pH values. These simple interpretations must be somewhat tempered, however, by the fact that ANS may also undergo electrostatic interactions with target proteins due to its negative charge.

Circular Dichroism Spectroscopy (CD). The thermal stability of the secondary structure of the RSV proteins was studied by CD. The CD spectra of RSV at low temperatures manifest minima near 208 and 222 nm over the entire pH range studied (spectra not shown). The wavelength positions of these minima suggest that the viral proteins contain a significant extent of α helical content. Contributions of the RNA to the CD signals do not appear to be large since characteristic CD bands above 240 nm are not seen. Furthermore, since similar spectra are obtained at low temperatures at each pH, significant disruptions of the secondary structure of the proteins do not appear to be induced by changes in pH alone. Upon heating, however, gradual losses in secondary structural content are observed at low temperatures from pH 3 to pH 5 (Figure 7). More abrupt losses in secondary structure are observed at pH 6−8 with the greatest secondary structural stability observed at pH 7. Overall, the CD data suggest that although significant alterations in viral protein secondary structure are not induced by pH changes alone, the secondary structural stability is optimized near neutral pH since the loss in the content of secondary structure is relatively minimal up to 40 °C at pH 7.

Dynamic Light Scattering (DLS). DLS was employed as a function of temperature to investigate the stability of the quaternary structure of RSV (Figure 8). The structural lability and tendency of RSV to aggregate below pH 6, however, prevented the use of DLS at pH 3−5. The average hydrodynamic diameter of RSV at low temperatures under neutral conditions was approximately 240 nm, and a polydispersity index of approximately 0.25 was observed reflecting the characteristic heterogeneous size distribution of RSV particles.

Although the mean hydrodynamic diameter of the virus remained relatively constant from 10 to 45 °C at pH 6, dramatic increases in the scattering rate and effective diameter were observed near 50 °C. Concomitant with these increases, an increase in the polydispersity index was observed suggesting an increase in the heterogeneity of the size distribution. These changes are consistent with the aggregation of the RSV particles observed during turbidity studies. Additionally, the temperatures at which these transitions take place correspond well with the onset of the structural transitions detected by the other techniques used in this work.

RSV undergoes a slight decrease in mean diameter at pH 7 and 8 prior to a moderate increase in size and intensity of scattered light, suggesting that these aggregated particles partially dissociate upon heating. The increases in scattering count rate near 55 °C correspond to increases in effective diameter and again correlate with the previously described increases in OD. These data confirm that RSV undergoes structural changes that lead to the extensive aggregation and observed increases in size of the viral particles under fairly moderate conditions.

An Empirical Phase Diagram (EPD) of RSV Temperature/pH Behavior. To provide a more intuitive and comprehensible picture of the behavior of RSV as it is

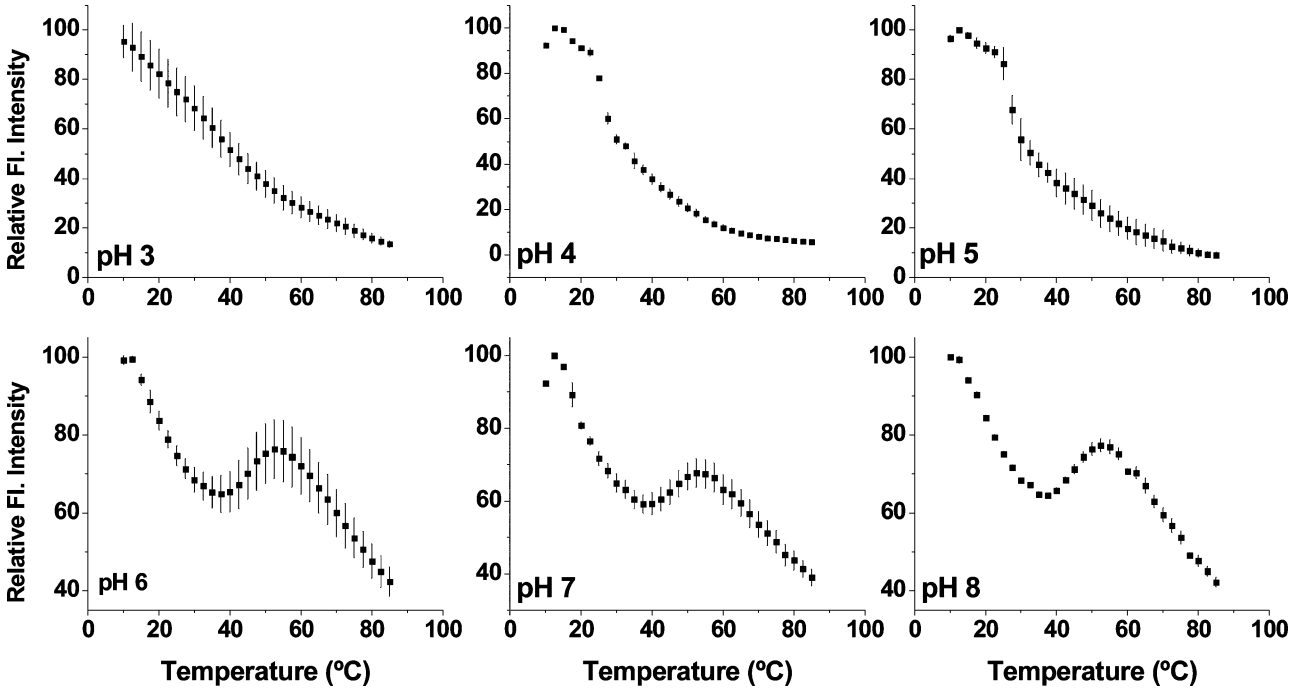

Figure 6. Relative extrinsic fluorescence intensity of ANS at 485 nm versus temperature for RSV (0.17 mg/mL protein) at pH 3−8 in 1 unit intervals.

stressed by temperature and pH, much of the data described in the previous sections was synthesized in the form of an empirical phase diagram (EPD) (Figure 9). This form of data presentation is not to be confused with a thermodynamic phase diagram in which equilibrium across phase boundaries is present. The colors observed can be thought of as vectors formed by the sum of colored components (red, green, and blue) which are derived from the individual experimental measurements. Since the EPD is generated by the incorporation of data based on measurements which are sensitive to the secondary, tertiary, and quaternary structure of RSV, regions of similar color reflect the range of temperature/pH conditions under which RSV is in a physically similar conformational state. Thus, as the temperature is increased, the conformational changes detected by the various techniques described above are manifested as color changes in the EPD. The red region in the EPD at low temperatures between pH 6 and 8 represents conditions under which the RSV proteins are in a conformationally similar state. Perturbations in the secondary, tertiary, and quaternary structure of the viral proteins that are detected above 40 °C, however, are manifested as a color change from red to green. The improved thermal stability at pH 7 and 8 is also evident since color changes in the EPD occur at higher temperatures. The data described in previous sections show that the secondary, tertiary, and quaternary structure of the RSV proteins is quite thermally labile and susceptible to aggregation under acidic conditions. Although the presence of aggregated viral particles at low temperature and low pH is manifested as discordant colors in the EPD, distinct structural changes that are detected in secondary, tertiary, and quaternary structure of the virus are still revealed.

Discussion

By the employment of a comprehensive biophysical characterization approach, we have shown that the secondary, tertiary, and quaternary structures of RSV are both pH and temperature labile. Second-derivative UV absorbance and fluorescence (intrinsic and extrinsic) spectroscopies suggest that the stability of tertiary structure of the RSV proteins is physically most stable at pH 7. Under neutral conditions, transitions in the tertiary structure are detected near 45 °C by UV absorbance and intrinsic fluorescence; however, conformational transitions are detected at slightly lower temperatures by changes in the fluorescence of the probe ANS. The initial fluorescence intensities of ANS are relatively high (Figure 6), suggesting that apolar environments are accessible to ANS even at low temperatures. Since RSV is an enveloped virus, it is plausible that ANS binds at low temperatures to the lipid membrane resulting in elevated fluorescence intensities. As the temperature is increased, the membrane may become more fluid and an enhancement in ANS fluorescence intensity is observed as a result of binding to the viral envelope. This binding, however, occurs prior to the detection of changes in protein conformation. When the transitions detected by absorbance and intrinsic fluorescence spectroscopies are taken into consideration, it seems possible that at least partial exposure of the hydrophobic regions of the transmembrane proteins (F, G, and SH)[12] gives rise to the initial structural changes detected by the tertiary structural sensitive methods. These transitions occur at higher temperatures than increases in membrane fluidity and allow increased binding of ANS to the hydrophobic regions of the transmembrane proteins. To investigate the stability of the viral envelope, extrinsic fluorescence spectroscopy was also

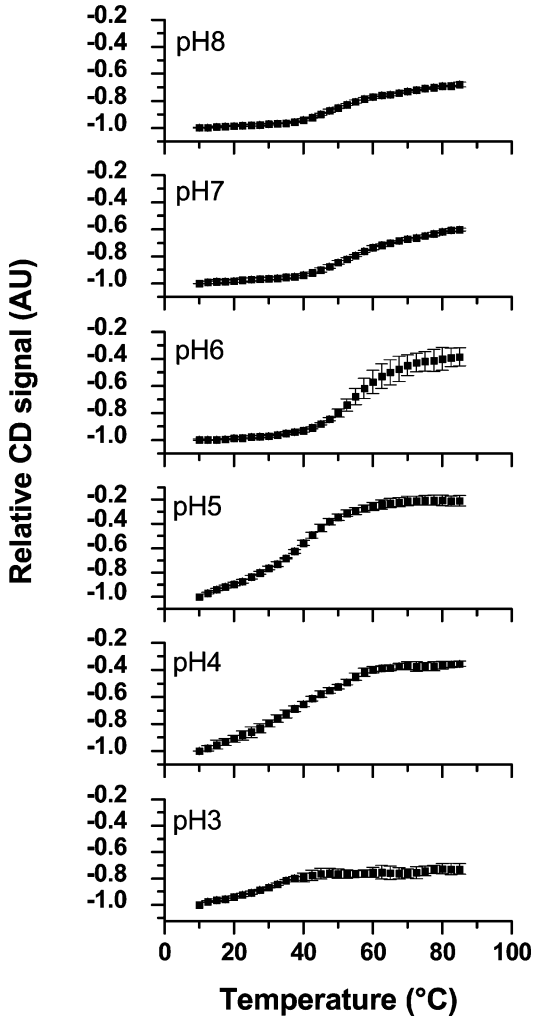

Figure 7. Relative CD signal at 222 nm as a function of temperature for RSV at pH 3−8.

conducted employing the extrinsic dye LAURDAN[22] (data not shown). Analysis of the membrane fluidity by this technique suggests that the lipid membrane is perturbed and more fluid at temperatures below those at which changes in the secondary and tertiary structure of the viral proteins are detected, supporting the hypothesis described above.

CD spectroscopy was used to evaluate the stability of the secondary structure of the RSV proteins. CD spectra of RSV at low temperatures suggest that the native form of the virus contains a significant degree of α helical content. Furthermore, Fourier transform infrared spectroscopy (FTIR) studies (data not shown) support the CD results and also suggest that the secondary structure of the RSV proteins is more stable under neutral solution conditions. These techniques also reveal that RSV proteins lose significant native secondary structural content below 40 °C at pH 3−5 and between 40 and 60 °C between pH 6 and 8. FTIR studies indicate that this is primarily due to the formation of intermolecular β sheets (i.e., aggregation). Since these secondary structural content and stability data correlate with transition temperatures obtained by the analysis of the tertiary and quaternary structural stability, these changes seem to be relatively cooperative in nature without clear evidence of molten globule-like intermediates.

Analysis of the quaternary structural stability and aggregation behavior of RSV by turbidity measurements and DLS also suggests that RSV is more thermally stable near neutral pH and particularly prone to aggregation below pH 6. In addition, increases in the optical density and scattering intensity near 50 °C suggest that the transitions detected by UV absorbance and fluorescence spectroscopies lead to the aggregation of the virus. The aggregated state of the virus at pH 3−5 hindered the application of DLS to investigate the more detailed behavior of viral quaternary structure with increasing temperature, but the elevated OD values observed at low temperatures compared to higher pH at low temperatures confirm the self-associative behavior of RSV at low pH.

When all of the data are combined into the form of an EPD, the physical stability of RSV and its lability under acidic conditions are readily apparent. In addition, the regions of color change in the EPD (i.e., empirical phase boundaries) identify conditions of temperature and pH where structural perturbations occur. Thus, conditions at the phase boundaries under which RSV shows intrinsic marginal stability can be used to select screening assays that in turn can be employed to identify stabilizers to inhibit or slow the individual degradation pathways responsible for the observed phase boundaries. Preliminary studies have identified several GRAS (generally regarded as safe) excipients using this approach. Although more work is needed to identify the mechanisms of stabilization and optimize the concentration of stabilizers, the use of this biophysical approach to identify physical degradation pathways and assess the structural stability of the virus can be employed for the rational design of a more thermally stable RSV vaccine. In addition to the pH−temperature EPD, supplementary stability studies under other solution conditions (i.e., ionic strength, osmolarity, etc.) could also be used to quickly generate phase diagrams and in this way obtain a more global picture of RSV stability.

This approach can be extended to other thermally labile viruses used in gene therapy, genetic vaccination, or conventional vaccines. For example, adenovirus has been successfully characterized by this approach.[18] Another immediate application may be to measles virus, which is also a member of the *Paramyxoviridae* family and therefore shares many structural similarities and lability issues with RSV. Measles continues to kill more than 500 000 people worldwide despite increased efforts by WHO and UNICEF to extend vaccination coverage throughout the developing world.[23,24] This high mortality rate has been attributed at least in part to the lack of a thermally stable measles vaccine and the inability to maintain a cold chain in remote parts of the globe. The application of biophysical characterization ap-

(22) Parasassi, T.; De Stasio, G.; Ravagnan, G.; Rusch, R. M.; Gratton, E. Quantitation of lipid phases in phospholipid vesicles by the generalized polarization of Laurdan fluorescence. *Biophys. J.* **1991**, *60*, 179−189.

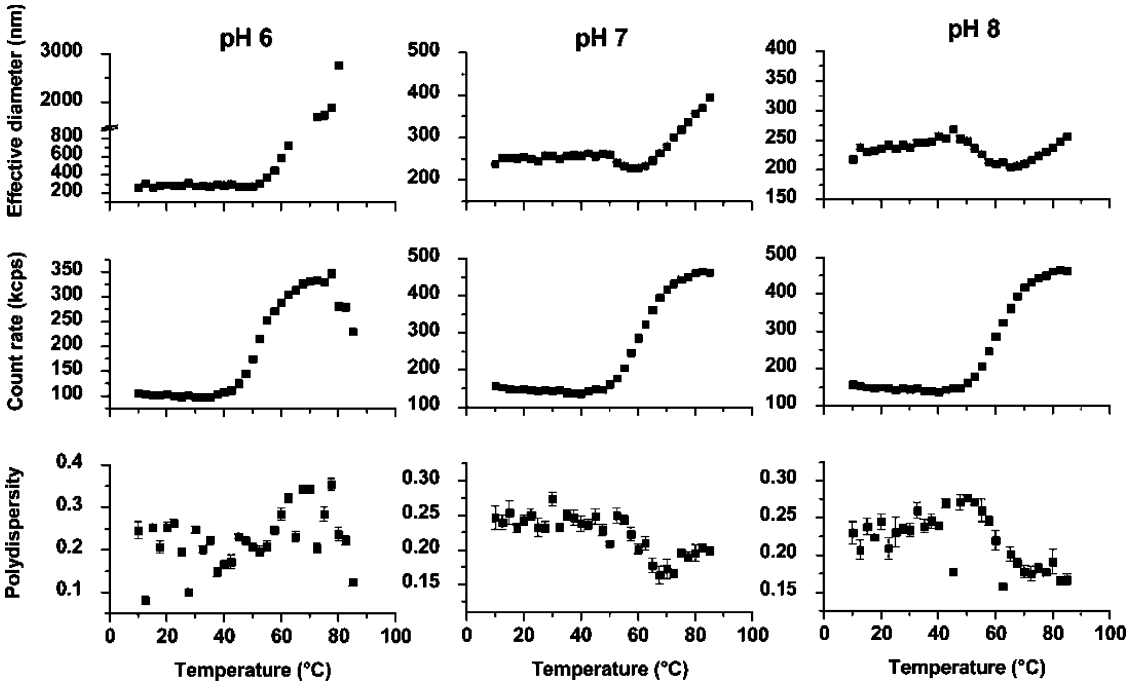

Figure 8. Quaternary structural analysis of RSV by dynamic light scattering over the pH range 6−8. Panels are arranged from top to bottom as effective diameter, scattering count rate, and polydispersity index, respectively.

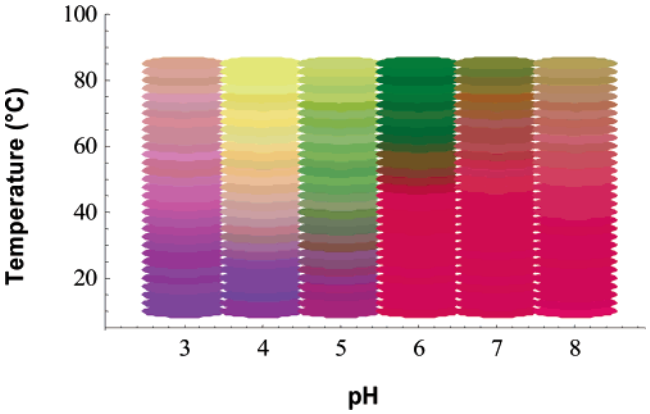

Figure 9. Empirical phase diagram (EPD) of RSV over the pH range 3−8. Data included in the generation of the EPD are all negative second-derivative UV peaks, CD signal at 222 nm, optical density at 350 nm, intrinsic fluorescence peak position, intrinsic fluorescence intensity at 330 nm, and ANS fluorescence intensity at 485 nm.

proach coupled to the rational design of a more thermally stable measles vaccine has the potential to facilitate increased vaccination coverage and lead to a dramatic decrease in mortality.

Although biophysical analyses have not previously been applied to assess the structural stability of intact RSV formulations, the physical stability data reported here do correlate well with biological activity studies conducted previously. For example, early efforts which focused on optimizing the biological activity of RSV following storage over a similar pH range found that the activity of RSV is lost at elevated rates if stored away from physiological pH.[13] Additionally, work by Rechsteiner showed that RSV is significantly thermolabile above 37 °C. A linear Arrhenius plot of the natural logarithm of viral activity versus $1/T$ also suggested that RSV undergoes a single mechanism of inactivation over the temperature range 37−50 °C.[14] Thus, since the physicochemical structure of any biological molecule or macromolecular complex such as a virus ultimately dictates its physiological effects, it seems plausible that the approach described here may be capable of detecting structural transformations within RSV that lead to inactivation of the virus. Ultimately, the inhibition of degradation pathways such as the ones identified herein should be a main focus in the rational design of a stable RSV vaccine. This raises the possibility of reducing the dependence on imprecise, time-consuming and inconvenient biological assays that are currently necessary to address stability problems.

Acknowledgment. This work was supported by Thrasher Research Fund Grant 02818-0 and Department of Defense Contract DAMD 17-03-C-0086.

MP0500465

(23) World Health Organization, United Nations Children's Fund. *Measles mortality reduction and regional elimination strategic plan 2001−2005;* World Health Organization: Geneva, Switzerland, 2001; available at http://www.who.int/vaccines-documents/docspdf01/www573.pdf.

(24) Centers for Disease Control and Prevention. Progress in Reducing Measles Mortality Worldwide, 1999−2003. *MMWR* **2005**, *54*, 200−203.